ELSEVIER

Materials Science and Engineering A 420 (2006) 155–164

MATERIALS SCIENCE & ENGINEERING A

www.elsevier.com/locate/msea

Infrared brazing of high-strength titanium alloys by Ti–15Cu–15Ni and Ti–15Cu–25Ni filler foils

C.T. Chang [a], Y.C. Du [a], R.K. Shiue [b,*], C.S. Chang [c]

[a] *Department of Materials Science and Engineering, National Dong Hwa University, Hualien 974, Taiwan*
[b] *Department of Materials Science and Engineering, National Taiwan University, Taipei 106, Taiwan*
[c] *Engineered Materials Solutions, 39 Perry Avenue, MS 4-1, Attleboro, MA 02703-2410, USA*

Received 20 June 2005; received in revised form 4 January 2006; accepted 17 January 2006

Abstract

Microstructures and fracture behaviors of infrared heated, vacuum brazed Ti–6Al–4V and Ti-15-3 alloys using two Ti–Cu–Ni braze fillers have been characterized to establish the effects of brazing process parameter and chemical composition on the strength of brazed joints. The brazed joint initially contains two prominent phases; a Ti alloy matrix alloyed with V, Cr, Ni, Cu and Al and a Cu–Ni-rich Ti phase. Brazing temperature and soak time control the amount of Cu–Ni-rich Ti phase in the brazed joints. The fracture mode changes from brittle cleavage to quasi-cleavage to ductile dimple as the amount of Cu–Ni-rich Ti phase is reduced in the brazed joint. Both brazing temperature and soak time are critical to eliminate the Cu–Ni-rich Ti phase for optimal shear strength and ductile fracture of brazed joints. A post-brazing annealing at lower temperature is also shown to be an effective way to homogenize the microstructure of brazed joint for improved joint strength.

Keywords: Infrared brazing; Ti–6Al–4V; Ti-15-3; Ti–15Cu–15Ni; Microstructure; Interface; Shear strength

1. Introduction

Titanium alloys are usually classified as α alloys, near-α alloys, α–β alloys and β alloys [1–3] based on the two allotropic phases, hexagonal low-temperature α phase and body-centered-cubic high-temperature β phase. The high-temperature β phase can be stabilized by alloy additions such as V and Mo.

The α–β alloys are used in aerospace application extensively, since the duplex microstructure can be tailored to provide either high toughness at ambient temperature or high creep resistance at elevated temperatures [1,4]. Ti–6Al–4V, a type of α–β alloy, is by far the most widely used titanium alloy, accounts for about 60% of the titanium market [1,2]. The composition of Ti–6Al–4V, in weight percent, contains the 6% Al as α phase stabilizer and 4% V as β phase stabilizer.

β-Titanium alloys have a number of attractive properties over other types of titanium alloys. β-Titanium alloys are fairly ductile and can be cold worked extensively. β-Titanium alloys can develop very high tensile strength from proper aging heat treatments [5]. Ti-15-3 alloy was developed during the 1970s and it was later scaled up to produce titanium strip [6]. The chemical composition of Ti-15-3 (also known as Ti-15-3-3-3) was developed to maintain stable β phase. It contains, in weight percent, 15% V, 3% Cr, 3% Al, 3% Sn and balance of Ti [5]. The strengthening mechanism of Ti-15-3 is generally attributed to the precipitation of uniformly dispersed fine α phase in the β-matrix [7,8]. The maximum tensile strength of Ti-15-3 can reach 1250 MPa when proper aging treatment is applied. It is used in various airframe applications, particularly in strip form.

Joining of Ti alloys has been extensively studied [9,10]. The commonly employed joining processes, welding, brazing and soldering, all face the demanding reactive nature of Ti alloys. The welding of titanium alloys has to be performed in inert gas or high-vacuum environment [2] with stringent process controls while brazing is accomplished with special braze alloys.

Brazing has been applied in joining of titanium alloys [11–15]. Brazing fillers for titanium alloy brazing can be divided into three groups: (1) Al-based, (2) Ag-based and (3) Ti-based alloys. Ti-based brazing fillers provide high joint strength and good corrosion resistance when compared to the other type of brazing fillers. Ti–15Cu–15Ni filler alloy is a commercially

* Corresponding author. Tel.: +886 2 33664533; fax: +886 2 23634562.
E-mail address: rkshiue@ntu.edu.tw (R.K. Shiue).

0921-5093/$ – see front matter © 2006 Elsevier B.V. All rights reserved.
doi:10.1016/j.msea.2006.01.046

available Ti-based brazing filler, its solidus and liquidus temperatures are 910 and 960 °C, respectively [15–18]. Ti–15Cu–25Ni alloy, with a higher Ni content and lower solidus and liquidus temperatures, was also studied to establish the effect of composition on the brazing of Ti alloys.

Commercial Ti-based braze fillers are available mostly in the powder form, even though foils have many obvious advantages, as it is not possible to obtain foils by the conventional metal working processes. A cold roll-bonding process was applied to combine Ti, Cu and Ni strip into a layered composite that allows conventional cold rolling process to produce the Ti–Ci–Ni brazing filler foils studied here [16].

The heating rate of traditional furnace brazing is usually operates at 10–30 °C/min. The very early stage of microstructural evolution in the brazed joint cannot be well analyzed due to its slow thermal history. In contrast, infrared vacuum brazing is characterized by a very high heating rate, which can be as high as 3000 °C/min. Accordingly, infrared brazing has been applied in many cases to characterize the effect of time and temperature on the microstructural evolution in the brazed joint [13–15]. With aid of the precisely controlled thermal history during brazing, the rapid heating and cooling capability of infrared process makes it a powerful tool in studying the microstructural evolution of the joint in brazing [19–24]. This information is very crucial in optimizing the process variables of brazing, e.g. brazing temperature, time and heating rate, etc. Additionally, a filler metal with a wide melting range needs rapid heating rates to minimize phase separation during brazing [17,18]. It is expected that the application of braze alloys is greatly increased for infrared brazing due to its rapid thermal cycles.

The objective of this investigation is to apply the precise control of infrared heating to study the microstructural evolution of two Ti–Cu–Ni fillers brazing Ti–6Al–4V and Ti-15-3 alloys. The microstructures of brazed joints and braze filler compositions will be rationalized with the shear strength tests and fractured surface observations. Conventional furnace brazed samples are also included to establish the correlation between two heating methods.

2. Experimental procedures

Commercial Ti–6Al–4V and Ti-15-3 plates measured 10 mm × 7 mm × 4 mm and 10 mm × 7 mm × 3 mm, respectively, were brazed for joint microstructure observation and shear strength evaluation, respectively. Brazed surfaces were polished with SiC papers up to 1200 grits and degreased in an ultrasonic bath of acetone [25]. Ti–15Cu–15Ni and Ti–15Cu–25Ni foils, 50 μm thick in as-rolled condition, consisting of layers of Ti, Cu and Ni were used as braze fillers.

The infrared brazing was performed in a vacuum of 5×10^{-5} mbar at 970, 1000, 1030 and 1060 °C for 180 and 300 s, respectively. The heating rate was kept at 600 °C/min throughout the experiment. The conventional furnace brazing was performed at 970 °C for 600, 1200 and 1800 s. The heating rate of conventional furnace brazing was kept at 30 °C/min. Post-brazing annealing at 900 °C for 3600 s was applied to some samples to characterize the microstructural evolution of brazed joints. Table 1 summarizes the brazing conditions used in this study and where the post-brazing annealing was applied.

Shear tests were employed in order to evaluate the joint strength of brazed specimen [22,26–28]. The shear test was performed using a Shimadzu AG-10 universal testing machine with a constant crosshead speed of 0.5 mm/min [22,26]. High-speed diamond saw was used to section metallography samples from the brazed coupons and shear test samples. Standard grinding and polishing sample preparation procedure was applied and Kroll's reagent (3 ml HF, 6 ml HNO_3 and 100 ml H_2O) [25] was used to delineate the microstructures.

Cross sections of brazed joint and fractured surface were examined by a scanning electron microscope (SEM), Hitachi 3500H, equipped with an energy-dispersive X-ray spectrometer (EDS) for chemical analysis. The operational voltage was kept at 20 kV and its minimum spot size was approximately 1 μm.

3. Results and discussion

3.1. Brazing Ti–6Al–4V and Ti-15-3 alloys using Ti–15Cu–15Ni filler metal

Fig. 1 shows SEM backscattered electron images (BEIs) and EDS chemical analysis results, in atomic percent, of infrared brazed Ti–6Al–4V/Ti–15Cu–15Ni/Ti-15-3 specimens with various brazing conditions. Firstly, the microstructure of brazed joint, even at the lowest brazing temperature 970 °C, after 180 s consists only of solidification microstructure without any indication that the filler foil has a layered structure prior to brazing. The microstructures of brazed joints changed greatly with higher brazing temperature or longer soak time. For specimen infrared brazed for 180 s at 970 °C, the brazed joint contains two readily resolvable phases. One is a darker Ti-rich phase alloyed with V, Cr, Ni, Cu and Al, which are marked by B, C, E and F in Fig. 1(a). The other phase is a light Ti-rich phase alloyed primarily with Cu and Ni, which is marked by A in Fig. 1(a). With increasing brazing temperature and/or time, the amount of light Ni–Cu-rich Ti phase is greatly decreased, and the dark Ti-rich phase eventually dominates the entire brazed joint as identified by G, H and J in Fig. 1(f).

The chemical composition of Ti–6Al–4V, in atomic percent, is 86.2% Ti, 10.2% Al and 3.6% V, and that of Ti-15-3 alloy is 76.4% Ti, 14.2% V, 2.8% Cr, 5.4% Al and 1.2% Sn. The chemical composition of Ti–15Cu–15Ni braze alloy is 74.8% Ti, 12.1% Cu and 13.1% Ni. It is obvious that both substrates are free of Cu and Ni and there is no Al, V, Cr and Sn in the filler metal.

Based on the EDS analysis, dissolution and interdiffusion between the braze filler and two substrates took place even at the lowest brazing temperature that indicates the propensity of this filler alloy on wetting the Ti alloys. The Ti–6Al–4V substrate shows signs of minor Cu and Ni dissolution as shown in D and I in Fig. 1(a and f). Both points F and H shows V dissolution and/or interdiffusion between Ti-15-3 substrate and the braze filler. It is also noted that the chemical composition of Ti–15Cu–15Ni (in atomic percent) is very close to that of light Cu–Ni-rich Ti phase

Table 1
Summary of the brazing process variables used in the experiment

Filler metal composition (wt%)	Type of brazing	Brazing time (s)	970 °C	1000 °C	1030 °C	1060 °C	Annealing temperature (°C)/time (s)
Ti–15Cu–15Ni	Infrared	180	S/M	S/M	S/M	S/M	
	Infrared	180	M				900/3600
	Infrared	300	M	M	M	M	
	Infrared	300			M		900/3600
	Furnace	600	M				
	Furnace	600	M				900/3600
	Furnace	1200	S/M				
	Furnace	1800	M				
Ti–15Cu–25Ni	Infrared	180	S/M	S/M	S/M	M	
	Infrared	180	S	S	S	M	900/3600
	Infrared	180	M	M	M	M	
	Infrared	180	M				900/3600

S: shear test specimen; M: metallographic specimen.

in the brazed joints. The rapid disappearing of this Cu–Ni-rich Ti phase as shown in Fig. 1(a–f) will play an important role in the strength and fracture behavior of brazed joint.

Based on the Cu–Ti and Ni–Ti binary alloy phase diagrams, the maximum solubility of Cu and Ni in β-Ti (13 and 10 at%) is much higher than that in α-Ti [29]. For the specimen infrared brazed at 970 °C for 180 s, the lowest brazing temperature and shortest soak time, there is significant amount of transient Cu–Ni-rich phase. When brazing temperature was raised to higher than 1000 °C, there is practically no trace of the Cu–Ni-rich phase observed as shown in Fig. 1.

Fig. 2 illustrates SEM images of furnace brazed Ti–6Al–4V/Ti–15Cu–15Ni/Ti-15-3 joints, in atomic percent, at 970 °C for 600, 1200 and 1800 s, respectively. Compared to the infrared brazed joint, the amount of Cu–Ni-rich phase, marked by A in Fig. 1(a) is greatly decreased due to the slow temperature ramping. Based on the EDS analysis results, Cu and Ni contents in the joint using furnace brazing (Fig. 2(a)) were significantly lower than those in the infrared brazed samples (Fig. 1). The Cu–Ni-rich phase disappeared all together in the furnace brazed specimen at 970 °C when soak time was longer than 1200 s.

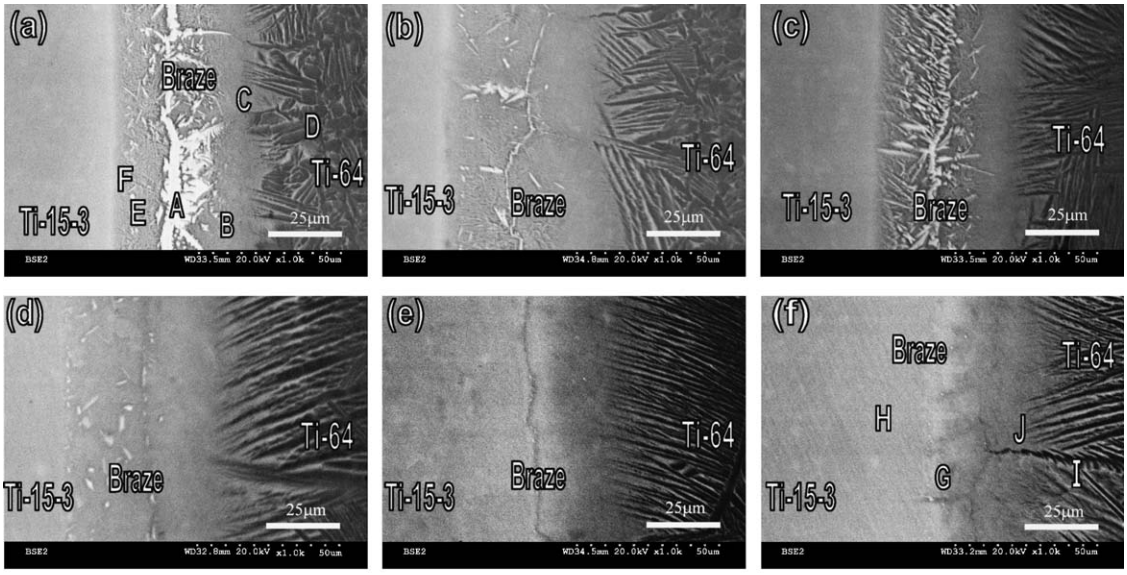

Location	A	B	C	D	E	F	G	H	I	J
Ti	69.5	81.5	81.1	85.7	74.2	76.6	81.7	79.4	81.9	84.1
V	0.8	1.9	2.3	2.2	2.7	9.9	5.6	9.0	4.0	3.2
Cr	0.1	0.3	0.2	0.0	0.4	1.7	0.8	1.4	0.0	0.3
Ni	12.1	5.9	5.3	0.8	8.1	3.1	3.3	2.6	2.7	3.0
Cu	15.6	6.0	5.3	0.4	11.8	3.1	3.8	2.5	1.7	3.3
Al	1.9	4.3	5.8	10.9	2.5	4.6	4.3	4.2	9.6	6.0
Sn	0.0	0.1	0.0	0.0	0.3	1.0	0.5	0.9	0.1	0.1

Fig. 1. SEM BEIs and EDS chemical analysis results, in atomic percent, of infrared brazed Ti–6Al–4V/Ti–15Cu–15Ni/Ti-15-3 specimens with various brazing conditions: (a) 970 °C × 180 s, (b) 970 °C × 300 s, (c) 1000 °C × 180 s, (d) 1000 °C × 300 s, (e) 1030 °C × 180 s and (f) 1030 °C × 300 s.

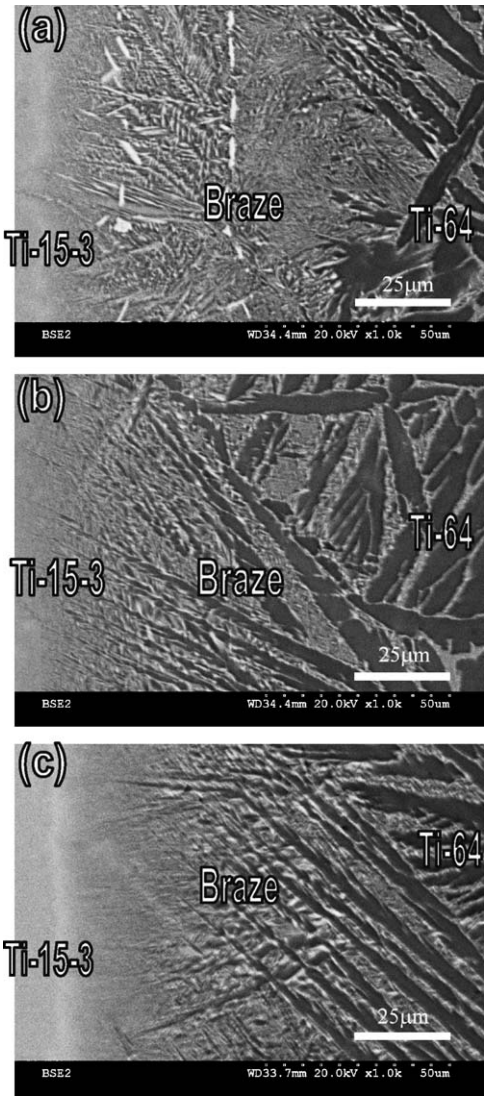

Fig. 2. The SEM images of furnace brazed Ti–6Al–4V/Ti–15Cu–15Ni/Ti-15-3 joints, in atomic percent, at 970 °C for (a) 600 s, BEI, (b) 1200 s, BEI and (c) 1800 s, BEI.

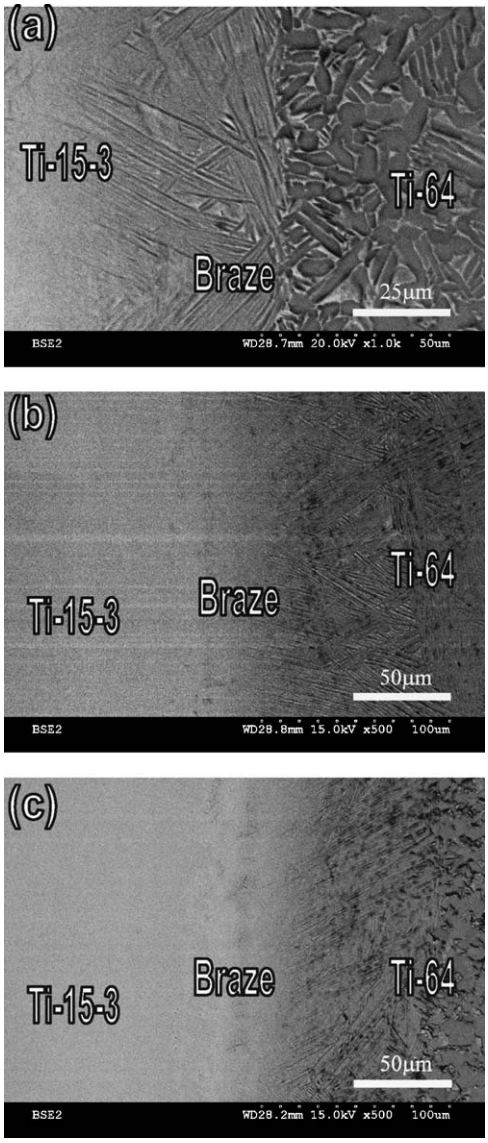

Fig. 3. The SEM images of post-braze annealed Ti–6Al–4V/Ti–15Cu–15Ni/Ti-15-3 joints, in atomic percent: (a) BEI, infrared brazed at 970 °C × 180 s, (b) SEI, infrared brazed at 1030 °C × 300 s, (c) SEI, furnace brazed at 970 °C × 600 s; all brazed specimens are annealed at 900 °C × 3600 s.

Table 2
Shear strengths of Ti–15Cu–15Ni brazed specimens

Brazing type	Temperature (°C)	Time (s)	Shear strength (MPa)	Average shear strength (MPa)
Furnace	970	1200	531	528
		1200	525	Fracture of substrate
Infrared	970	180	306	303
		180	300	303
Infrared	1000	180	448	452
		180	456	Fracture of substrate
Infrared	1030	180	463	470
		180	477	Fracture of substrate
Infrared	1060	180	506	511
		180	515	Fracture of substrate

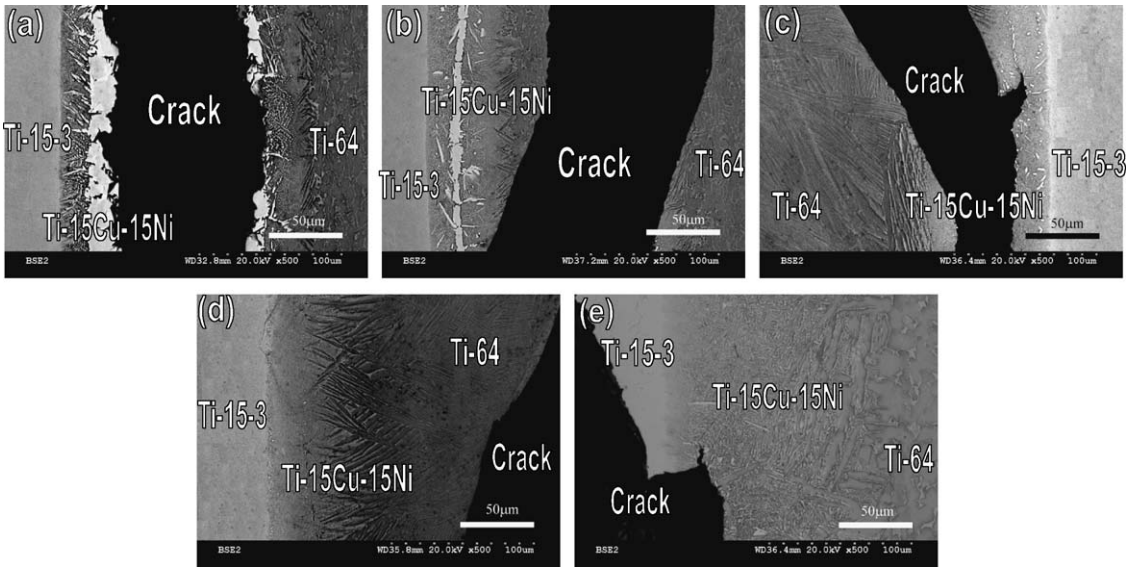

Fig. 4. SEM BEIs illustrate the cross section of brazed Ti–6Al–4V/Ti–15Cu–15Ni/Ti-15-3 joints after shear test: (a) infrared brazing, 970 °C × 180 s, (b) infrared brazing, 1000 °C × 180 s, (c) infrared brazing, 1030 °C × 180 s, (d) infrared brazing, 1060 °C × 180 s and (e) furnace brazing, 970 °C × 1200 s.

Fig. 3 shows SEM images of infrared and furnace brazed specimens with an additional post-braze annealing at 900 °C for 3600 s. It is clear that both Cu and Ni contents in the brazed joints decreased significantly due to the huge solubility of these elements in β-Ti. The ready assimilation of brazed joint is significant in order to obtain the joint with properties that are identical to the substrate materials. The effect of large amount of raising Ni and Cu elements in Ti-15-3 or Ti–6Al–4V is not clear at this point and further studies are underway.

Table 2 shows the shear strength of Ti–15Cu–15Ni brazed specimens with various brazing conditions. Most of the shear specimens fractured though the substrate except the 970 °C, 180 s infrared brazed sample. Fig. 4 displays the SEM BEIs of cross sections of shear tested Ti–6Al–4V/Ti–15Cu–15Ni/Ti-15-3 brazed joints with different brazing conditions. It is obvious that the 970 °C, 180 s infrared brazed sample fractured along the brazed joint as demonstrated in Fig. 4(a). With increasing brazing temperature and/or soak time, the fracture path changed from the brazed joint into the substrate as demonstrated in Fig. 4(b–e).

Fig. 5 shows SEM fractographs of Ti–6Al–4V/Ti–15Cu–15Ni/Ti-15-3 braze joints under shear with various brazing conditions. Brittle cleavage fracture dominated the 970 °C, 180 s infrared brazed sample (Fig. 5(a)). The fractured morphology changed from cleavage to quasi-cleavage in specimen infrared brazed at temperature above 1000 °C for 180 s (Fig. 5(b–d)). Dimple rupture fracture virtually covered the entire fractured surface of specimen furnace brazed at 970 °C for 1200 s (Fig. 5(e)).

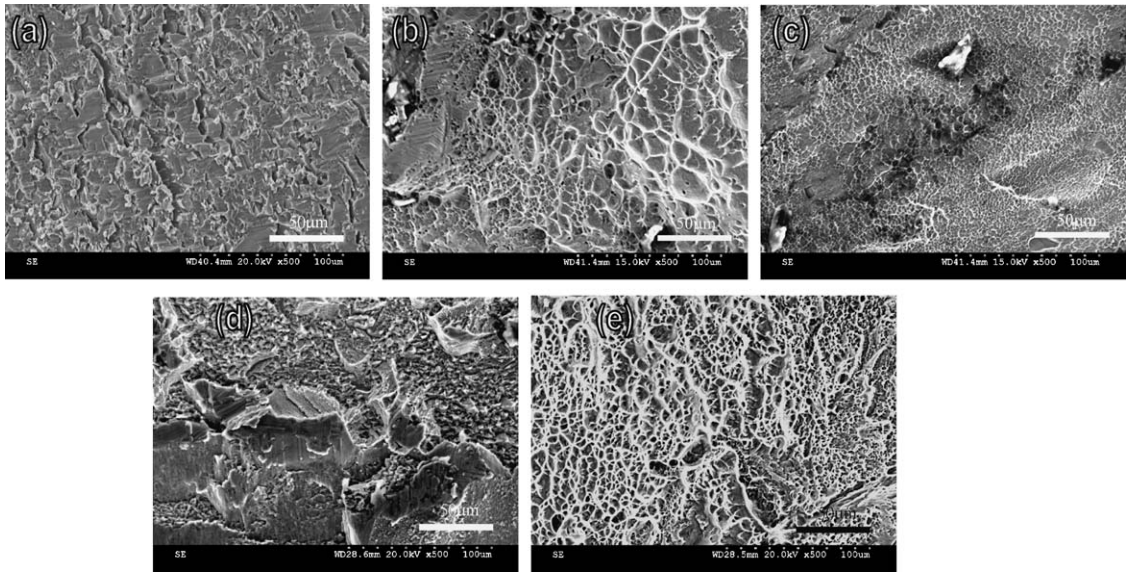

Fig. 5. SEM fractographs of the brazed Ti–6Al–4V/Ti–15Cu–15Ni/Ti-15-3 specimens after the shear test: (a) infrared brazing, 970 °C × 180 s, (b) infrared brazing, 1000 °C × 180 s, (c) infrared brazing, 1030 °C × 180 s, (d) infrared brazing, 1060 °C × 180 s and (e) furnace brazing, 970 °C × 1200 s.

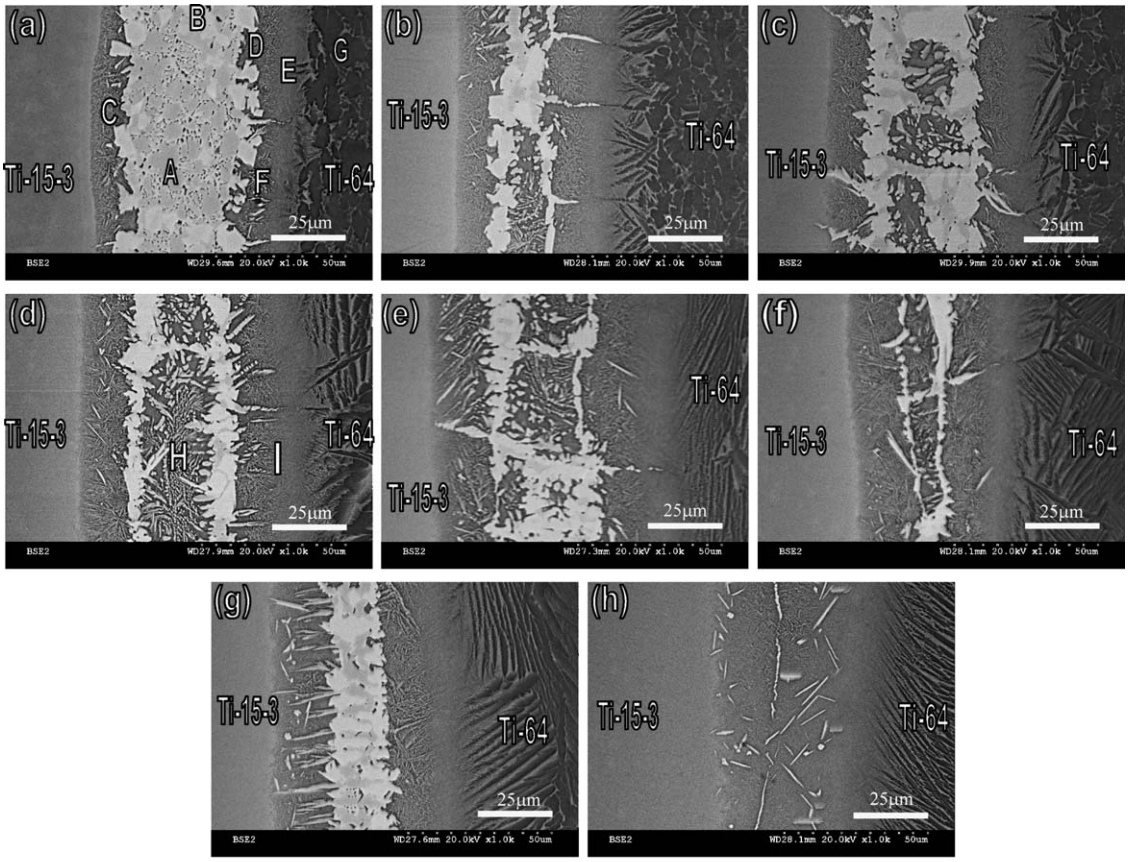

Location	A	B	C	D	E	F	G	H	I
Ti	67.9	69.1	78.0	78.6	80.0	79.1	87.2	75.9	80.3
V	0.3	2.2	4.2	2.4	2.9	2.0	1.9	2.6	3.1
Al	0.9	2.1	2.9	3.7	6.5	3.9	10.5	2.8	6.0
Ni	15.1	19.8	6.8	7.8	6.1	7.8	0.2	9.7	6.1
Cu	15.5	6.4	6.7	7.0	4.3	6.7	0.2	8.6	4.3
Cr	0.2	0.2	0.7	0.3	0	0.3	0	0.3	0.2
Sn	0.1	0.2	0.7	0.2	0.2	0.2	0	0.1	0.0

Fig. 6. SEM BEIs and EDS chemical analysis results of infrared brazed Ti–6Al–4V/Ti–15Cu–25Ni/Ti-15-3 specimens, in atomic percent, with various brazing conditions: (a) 970 °C × 180 s, (b) 970 °C × 300 s, (c) 1000 °C × 180 s, (d) 1000 °C × 300 s, (e) 1030 °C × 180 s, (f) 1030 °C × 300 s, (g) 1060 °C × 180 s and (h) 1060 °C × 300 s.

The fracture mode modification, shear test results and microstructural observations of the joint indicate that the presence of Cu–Ni-rich phase reduces both the strength and the ductility of brazed joint. Accordingly, it is critical to apply appropriate brazing process parameters, e.g. brazing time and temperature, to reduce or eliminate the presence of Cu–Ni-rich Ti phase in the joint. It is essential to obtain the desirable joint strength and toughness for engineering structural applications.

3.2. Brazing Ti–6Al–4V and Ti-15-3 alloys using Ti–15Cu–25Ni filler metal

Fig. 6 shows SEM BEIs and EDS chemical analysis results of infrared brazed Ti–6Al–4V/Ti–15Cu–25Ni/Ti-15-3 specimens, in atomic percent, with various brazing conditions. In contrast to Ti–15Cu–15Ni filler metal, the amount of Cu–Ni-rich phase in the Ti–15Cu–25Ni brazed joint is much higher and persist to higher brazing temperatures or longer soak time as shown in Fig. 6. Furthermore, both Cu and Ni concentrations in the Cu–Ni-rich phase are higher than those in the Ti–15Cu–15Ni brazed joint as marked by A and B in Fig. 6. The amount of Cu–Ni-rich phase in the brazed joint was reduced significantly in specimen infrared brazed at 1060 °C for 300 s (Fig. 6(h)).

Fig. 7 illustrates the SEM images and EDS chemical analysis results of Ti–6Al–4V/Ti–15Cu–25Ni/Ti-15-3 brazed joints, in atomic percent, with post-brazing annealing at 900 °C for 3600 s. The Cu–Ni-rich phase is virtually eliminated and the contents of Cu and Ni in braze joint decrease significantly as demonstrated in Fig. 7(a). A post-brazing annealing treatment is more effective to improve the joint strength as shown in Table 3, which tabulates the shear strength of Ti–15Cu–25Ni brazed specimens. Specimen infrared brazed at 970 °C for 180 s without any further heat treatment shows low average shear strength of 282 MPa. The average shear strength increases from

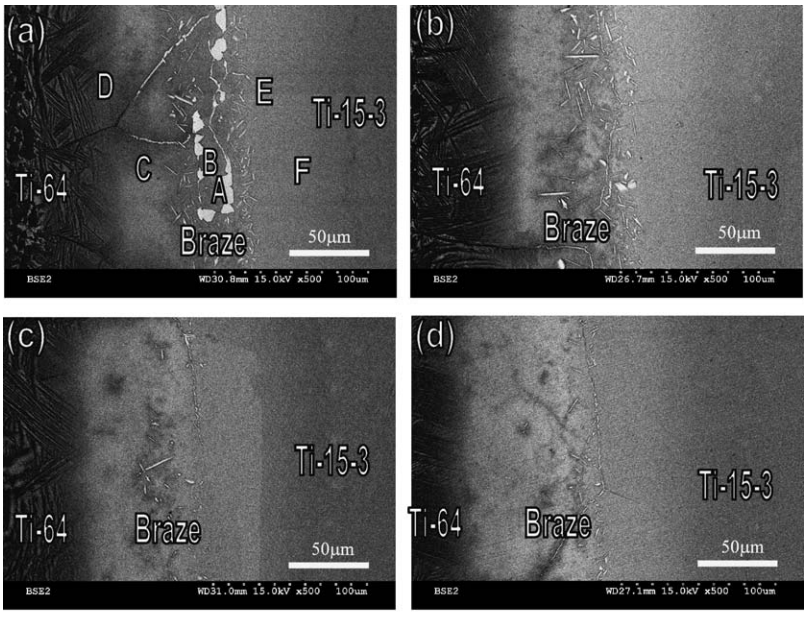

Location	A	B	C	D	E	F
Ti	73.2	80.2	79.7	76.8	77.1	73.8
Al	2.7	7.2	10.0	12.5	7.0	7.9
V	0.1	3.7	2.6	3.5	7.5	12.0
Cu	3.6	2.7	2.7	2.3	2.0	0.7
Ni	19.9	5.2	4.5	4.7	4.5	1.9
Cr	0.3	0.6	0.3	0.0	1.0	2.3
Sn	0.2	0.4	0.2	0.2	0.9	1.4

Fig. 7. The SEM BEIs and EDS chemical analysis results of post-brazing annealed Ti–6Al–4V/Ti–15Cu–25Ni/Ti-15-3 joints, in atomic percent: (a) infrared brazed at 970 °C × 180 s, (b) infrared brazed at 970 °C × 300 s, (c) infrared brazed at 1000 °C × 180 s and (d) infrared brazed at 1030 °C × 180 s; all brazed specimens are annealed at 900 °C × 3600 s.

282 to 410 MPa with increasing infrared brazing temperature (from 970 to 1030 °C). A post-brazing annealing of 900 °C for 3600 s greatly increased the shear strength of all brazed specimens. The maximum average shear strength of Ti–15Cu–25Ni brazed specimen is 545 MPa, which is comparable to that of specimen brazed with Ti–15Cu–15Ni.

Fig. 8 shows cross sections of Ti–15Cu–25Ni brazed specimens after shear test. All specimens failed along the Cu–Ni-rich phase in the as-brazed condition. Fig. 9 shows SEM fractographs of as-brazed Ti–6Al–4V/Ti–15Cu–25Ni/Ti-15-3 specimens after the shear test for different brazing conditions. Fractured surfaces are dominated by brittle cleavages and there

Table 3
Shear strengths of Ti–15Cu–25Ni brazed specimens

Brazing type	Temperature (°C)	Time (s)	Annealing temperature (°C)/time (s)	Shear strength (MPa)	Average shear strength (MPa)
Infrared	970	180	–	294	282
		180	–	268	
Infrared	970	180	900/3600	417	437
		180	900/3600	457	
Infrared	970	300	900/3600	471	473
		300	900/3600	475	
Infrared	1000	180	–	369	348
		180	–	328	
Infrared	1000	180	900/3600	493	496
		180	900/3600	499	
Infrared	1030	180	–	424	410
		180	–	395	
Infrared	1030	180	900/3600	542	545
		180	900/3600	547	

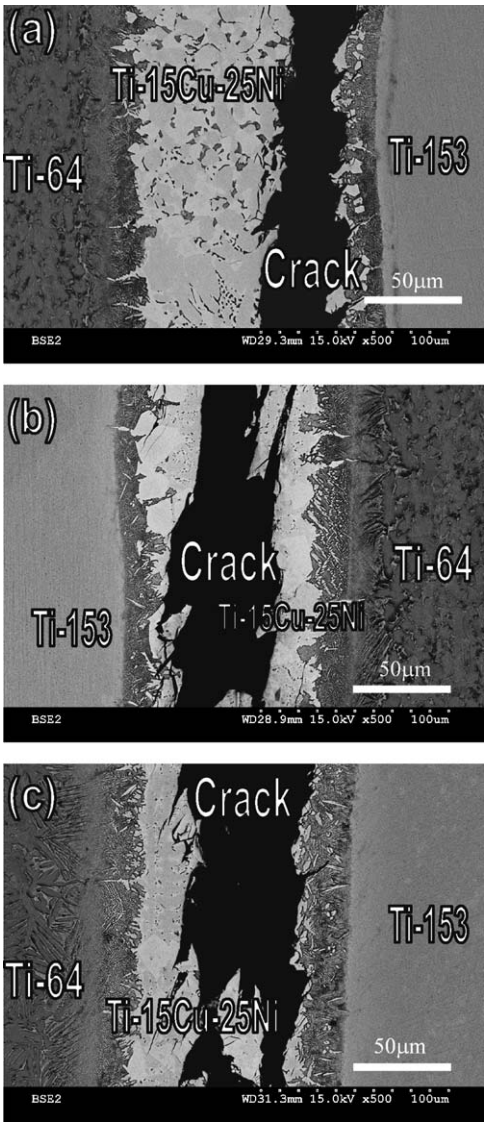

Fig. 8. SEM BEIs illustrate the cross section of brazed Ti–6Al–4V/Ti–15Cu–25Ni/Ti-15-3 joints after shear test: (a) infrared brazing, 970 °C × 180 s, (b) infrared brazing, 1000 °C × 180 s and (c) infrared brazing, 1030 °C × 180 s.

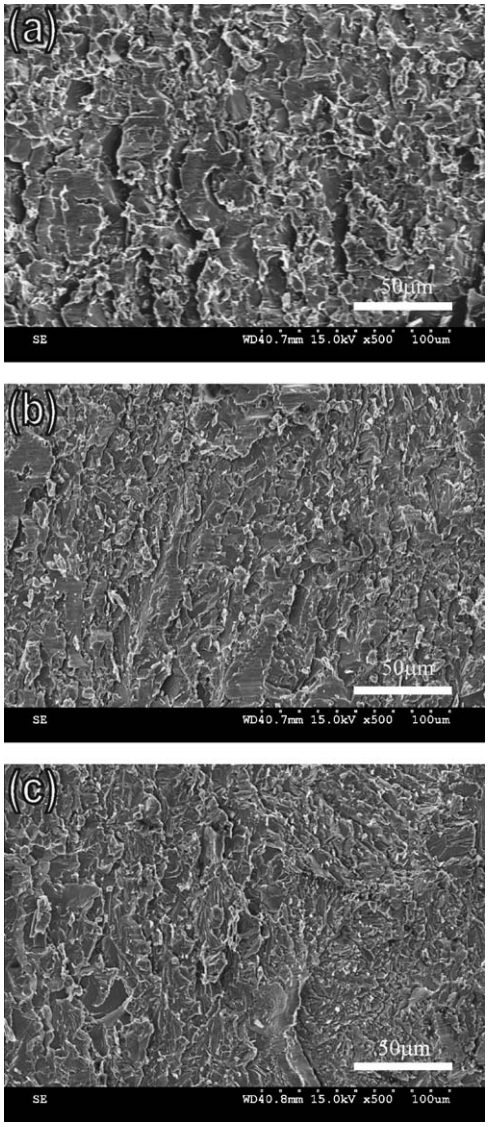

Fig. 9. SEM fractographs of the brazed Ti–6Al–4V/Ti–15Cu–25Ni/Ti-15-3 specimens after the shear test: (a) infrared brazing, 970 °C × 180 s, (b) infrared brazing, 1000 °C × 180 s and (c) infrared brazing, 1030 °C × 180 s.

is no ductile dimple fracture to be found. It demonstrates that the presence of Cu–Ni-rich phase is detrimental to the strength of all brazed joints.

Fig. 10 shows the cross sections and EDS chemical analysis of post-brazing annealed joints subjected to shear test. In contrast to the brazed joint using Ti–15Cu–15Ni filler metal, the fractured path primarily propagated along the brazed joint. Fig. 11 shows SEM fractographs of post-brazing annealed Ti–6Al–4V/Ti–15Cu–25Ni/Ti-15-3 shear specimens. The fractured morphology is very different as compared between Figs. 9 and 11. For specimens without post-brazing annealing, the fractured surfaces are dominated by brittle cleavages and there is no ductile dimple fracture to be found as illustrated in Fig. 9. Quasi-cleavage fracture is observed in the post-brazing annealed infrared brazed specimen at 970 °C for 180 s (Fig. 11(a)), while dimple fractures are widely observed in other samples that were infrared brazed at higher temperature and/or longer time (Fig. 11(b–d)).

3.3. Braze joint properties and braze filler compositions

It is well established that the brazed joint fractured in a ductile dimple manner is preferred to that in a quasi-cleavage or cleavage manner. This study has shown that the type of fractured joint depends on the presence of Cu–Ni-rich phase.

For the two Ti–Cu–Ni-based braze fillers studied here, a ductile dimple fracture is readily obtainable when Ni and Cu contents in the filler alloy are lowered. Infrared brazed samples showed transition from cleavage fracture with low shear strength to dimple ductile fracture through the substrate alloys when sufficiently high temperature and/or longer soak time was applied to the Ti–15Cu–15Ni filler. The transition was barely noticeable in samples infrared brazed with Ti–15Cu–25Ni filler even

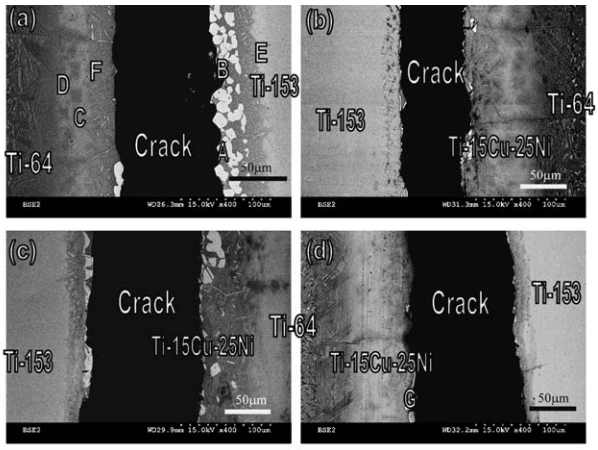

Location	A	B	C	D	E	F	G
Ti	73.2	76.4	79.5	77.8	75.3	76.5	72.2
Al	1.7	5.1	10.2	13.7	6.7	8.5	2.0
V	0.4	4.1	2.5	2.8	10.3	2.2	0.8
Cu	4.8	7.3	3.1	2.4	2.0	6.0	4.5
Ni	19.3	5.3	4.4	3.1	3.0	5.6	19.9
Cr	0.5	0.9	0.2	0.0	1.5	0.5	0.3
Sn	0.1	0.9	0.1	0.2	1.2	0.7	0.3

Fig. 10. SEM BEIs displaying the cross section of post-brazing annealed Ti–6Al–4V/Ti–15Cu–25Ni/Ti-15-3 joints after shear test and EDS chemical analysis: (a) infrared brazing, 970 °C × 180 s, (b) infrared brazing, 970 °C × 300 s, (c) infrared brazing, 1000 °C × 180 s and (d) infrared brazing, 1030 °C × 180 s; all brazed specimens are annealed at 900 °C × 3600 s.

at the highest brazing temperature. It is important to note that, as shown in this study, an additional post-brazing annealing at temperatures above β-transus was sufficient to homogenize most of the infrared brazed joint areas and to obtain ductile brazed joint with higher shear strength.

Cu and Ni are added as the melting point depressants (MPDs) in the Ti–Cu–Ni family of brazing filler alloys [17,18,30,31]. In the brazing of Ti alloy, it is critical that the brazing temperature should be kept as low as possible to avoid significant α–β phase transformation, which can adversely affect the mechanical properties of Ti alloy substrates. α–β phase transformation manifests differently in an α–β Ti alloy from that in a β-Ti alloy. Excessively high brazing temperatures cause α phase to precipitate along the β grain boundaries in a β-Ti alloy to embrittle the substrate. For an α–β Ti alloy, excessively high brazing temperatures might alter the carefully designed two-phase microstructure sufficiently to render the substrate useless. This study shows that the contents of Cu and Ni in the brazed joint can be greatly decreased by a properly designed brazing and post-brazing heat treatment. For selection of a Ti-based braze alloy, the one with lower brazing temperature, i.e. higher MPDs, is not always beneficial since the additional post-brazing heat

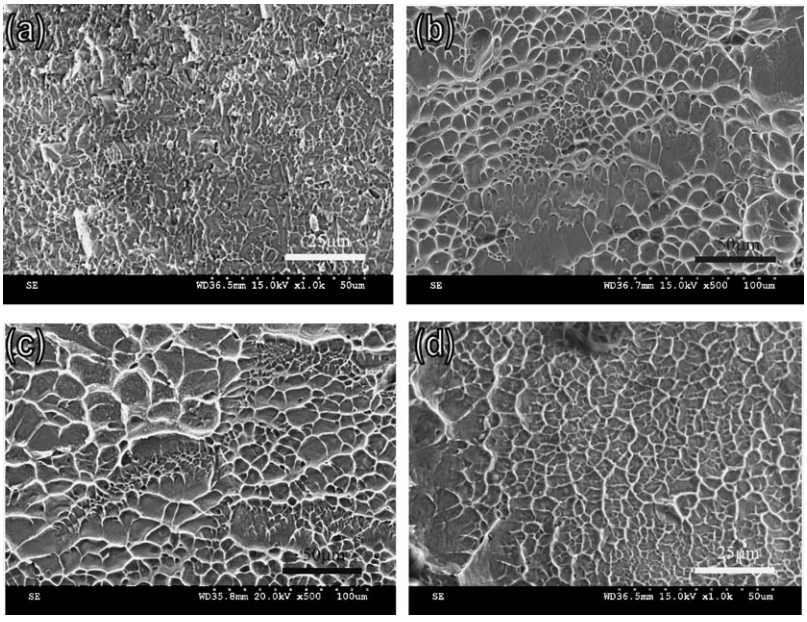

Fig. 11. SEM fractographs of post-braze annealed Ti–6Al–4V/Ti–15Cu–25Ni/Ti-15-3 specimens after the shear test: (a) infrared brazing, 970 °C × 180 s, (b) infrared brazing, 970 °C × 300 s, (c) infrared brazing, 1000 °C × 180 s and (d) infrared brazing, 1030 °C × 180 s; all brazed specimens are annealed at 900 °C × 3600 s.

treatment might cause microstructural degradation or embrittlement of the Ti alloy substrates.

4. Conclusions

The brazing of two high-strength titanium alloys using Ti–15Cu–15Ni and Ti–15Cu–25Ni filler foils are characterized in the experiment. Important conclusions are summarized as below:

(1) Brazed joints from lower brazing temperature and shorter soak time contain at least two phases. One is a Ti-rich phase with V, Cr, Ni, Cu and Al and the other is a Cu–Ni-rich phase. Increasing the brazing temperature and/or time results in decreasing the Cu–Ni-rich Ti phase, which is eventually disappeared in the ductile Ti matrix.
(2) In general, the average shear strength increases with increasing infrared brazing temperature and/or time. The average shear strength is further increased for all brazed specimens when a post-brazing annealing is applied.
(3) The fracture mode of shear test sample changes from brittle cleavage to quasi-cleavage to ductile dimple as the brazing temperature and time increases. The presence of Cu–Ni-rich phase corresponds with the low shear strength and brittle fracture of the brazed joint.
(4) The contents of Cu and Ni in the brazed joint can be greatly decreased by properly implemented brazing and post-brazing annealing treatment. The higher the Cu and/or Ni contents in the braze alloy, the higher brazing temperature and/or longer brazing time are required to homogenize the microstructure of the joint. Additionally, post-brazing annealing is found to be an alternative method to avoid a long soak time at high brazing temperature.

Acknowledgement

The authors gratefully acknowledge the financial support of this study by National Science Council (NSC), Republic of China, under NSC grants 93-2216-E-002-028.

References

[1] J.A. Jacobs, Engineering Materials Technology, Prentice-Hall International Inc., New York, 1997, p. 301.
[2] W.F. Smith, Structure and Properties of Engineering Alloys, McGarw-Hill Inc., New York, 1993, p. 433.
[3] J.R. Davis, ASM Handbook, vol. 2, ASM International, Materials Park, 1990.
[4] J.L. Walter, M.R. Jackson, C.T. Sims, Titanium and its Alloys: Principles of Alloying Titanium, ASM International, Metals Park, 1988.
[5] O.P. Karasevskaya, O.M. Ivasishin, S.L. Semiatin, Yu.V. Matviychuk, Mater. Sci. Eng. A354 (2003) 121.
[6] R. Boyer, E.W. Collings, G. Welsch, Materials Properties Handbook: Titanium Alloys, ASM International, Materials Park, 1994.
[7] S.J. Kim, B.H. Choe, Y.T. Lee, in: S. Fujishiro, et al. (Eds.), Metallurgy and Technology of Practical Ti Alloys, TMS, Warrendale, PA, 1994, p. 167.
[8] M. Jimin, Q. Wang, Mater. Sci. Eng. A243 (1998) 150.
[9] M. Ishikawa, O. Kuboyama, M. Niikura, C. Ouchi, Titanium'92: Science and Technology, vol. 2, TMS, Warrendale, 1993, p. 141.
[10] T. Fujita, M. Ishikawa, S. Hashimoto, K. Minakawa, C. Ouchi, in: D. Eylon (Ed.), Beta Titanium Alloy in the 1990s, TMS, Warrendale, 1993, p. 61.
[11] M.S. Tucker, K.R. Wilson, Welding J. 48 (12) (1969) 521s.
[12] N.A. Dececco, J.N. Parks, Welding J. 32 (1953) 1071.
[13] C.T. Chang, R.K. Shiue, C.S. Chang, Scripta Mater. 54 (2006) 853.
[14] H.Y. Chan, D.W. Liaw, R.K. Shiue, Int. J. Refract. Met. Hard Mater. 22 (2004) 27.
[15] T.Y. Yang, R.K. Shiue, S.K. Wu, Intermetallics 12 (2004) 1285.
[16] C.S. Chang, B. Jha, Welding J. 82 (10) (2003) 28.
[17] D.L. Olson, T.A. Siewert, S. Liu, G.R. Edwards, ASM Handbook, vol. 6, Welding, Brazing and Soldering, ASM International, Materials Park, 1993.
[18] G. Humpston, D.M. Jacobson, Principles of Soldering and Brazing, ASM International, Materials Park, 1993.
[19] Y.L. Lee, R.K. Shiue, S.K. Wu, Intermetallics 11 (2003) 187.
[20] R.K. Shiue, S.K. Wu, C.M. Hung, Metall. Mater. Trans. 33A (2002) 1765.
[21] T.Y. Yang, S.K. Wu, R.K. Shiue, Intermetallics 9 (2001) 341.
[22] R.K. Shiue, S.K. Wu, S.Y. Chen, Acta Mater. 51 (2003) 1991.
[23] C.L. Ou, R.K. Shiue, J. Mater. Sci. 38 (2003) 2337.
[24] C.C. Liu, C.L. Ou, R.K. Shiue, J. Mater. Sci. 37 (2002) 2225.
[25] G.F. Vander Voort, Metallography Principle and Practice, McGarw-Hill Inc., New York, 1984.
[26] R.K. Shiue, S.K. Wu, C.M. Hung, Metall. Mater. Trans. 33A (2002) 1765.
[27] Y. Hiraoka, Int. J. Refract. Met. Hard Mater. 11 (1992) 303.
[28] Y. Hiraoka, S. Nishikawa, Int. J. Refract. Met. Hard Mater. 14 (1996) 311.
[29] T.B. Massalski, Binary Alloy Phase Diagrams, ASM International, Materials Park, 1990.
[30] P. Villars, A. Prince, H. Okamoto, Handbook of Ternary Alloy Phase Diagrams, ASM International, Materials Park, 1995.
[31] A. Shapiro, A. Rabinkin, Welding J. 82 (10) (2003) 36.